JOURNAL OF APPLIED ELECTROCHEMISTRY **27** (1997) 1149–1156

Influence of gas phase mass transfer limitations on molten carbonate fuel cell cathodes

E. FONTES, C. LAGERGREN, G. LINDBERGH, D. SIMONSSON

Department of Chemical Engineering and Technology, Applied Electrochemistry, Kungliga Tekniska Högskolan (KTH), SE-100 44 Stockholm, Sweden

Received 25 November 1996; revised 10 February 1997

The purpose of this paper is to elucidate to what extent mass transfer limitations in the gas phase affect the performance of porous molten carbonate fuel cell cathodes. Experimental data from porous nickel oxide cathodes and calculated data are presented. One and two-dimensional models for the current collector and electrode region have been used. Shielding effects of the current collector are taken into account. The mass balance in the gas phase is taken into account by using the Stefan–Maxwell equation. For standard gas composition and normal operating current density, the effect of gas-phase diffusion is small. The diffusion in the gaseous phase must be considered at operation at higher current densities. For low oxygen partial pressures, the influence of mass transfer limitations is large, even at low current densities. To eliminate the influence of conversion on polarization curves recorded on laboratory cell units, measurements should always be performed with a five to tenfold stoichiometric excess of oxygen. Two-dimensional calculations show rather large concentration gradients in directions parallel to the current collector. However, the influence on electrode performance is still small, which is explained by the fact that most of the current is produced close to the electrolyte matrix.

Keywords: *Electrode performance, Fuel cell, Gaseous diffusion, Mass transfer, Porous cathode*

1. Introduction

The molten carbonate fuel cell (MCFC) is, due to its highly efficient and clean conversion of chemical energy into electric energy, of great interest for future power generation. As with most other fuel cell systems the cathode is a major source of cell polarization. The state-of-the-art cathode in the molten carbonate fuel cell is an *in situ* lithiated and oxidized NiO electrode, which gradually dissolves in the electrolyte used. Although the instability of the NiO cathode is a problem, the dissolution rate may be kept at an acceptable level by control of the operating conditions.

Several factors may affect the cathode performance: the electrochemical activity of the electrode material as well as the design parameters of the porous electrode. The kinetics for the oxygen reduction in the cathode have been much researched [1–3]. However, since the reaction mechanism is still unknown several kinetic parameters remain to be determined. With regard to the porous electrode properties, electrode thickness, porosity and electrolyte filling are some of the factors influencing the cathode performance.

Important to the design of the electrode is the transfer of the reacting species from the incoming gas to the electroactive areas inside the electrode. Both the mass transfer within the electrolyte film and in the gaseous phase are factors to be taken into account when looking at cathode performance. In general, the influence of mass transfer in the electrolyte has been judged to have a much larger influence on the electrode performance than mass transfer limitations in the gaseous phase. However, balance of plant calculations and the practical operation of pilot plant units have shown that the actual pressure of oxygen and carbon dioxide in the oxidant gas could be well below 0.10 atm, especially at outlet conditions in the stack. Economic considerations will probably increase the average current density for operation of future stacks from today's 1500 $A\,m^{-2}$. These operating conditions will result in a larger influence of gas phase mass transfer limitations in the system. One possible improvement of the performance of a cell would be to increase the total pressure and thereby reduce the influence of mass transfer limitations. This will, however, drastically decrease the life of the nickel oxide cathode and, at present, operation at atmospheric or moderately increased pressures seems to be more realistic.

To elucidate gas-phase diffusional losses, Yuh and Selman [1] replaced the inert gas nitrogen by helium. They concluded that the inert gas had little effect on the cathode performance, that is, the gas-phase mass transfer resistance can be neglected. However, their experiments with helium included only the gas composition with 15% O_2 and 30% CO_2 and current

0021-891X

densities less than about $1550\,A\,m^{-2}$. Nevertheless, already at this current density, corresponding to normal operation conditions, a small effect may be observed. In contrast to the conclusion of Yuh and Selman, Bregoli and Kunz [4] claimed that there are considerable gas-phase mass transfer limitations when using nitrogen as an inert gas. Weaver and Winnick [5] studied the performance of the MCFC cathode at extremely low carbon dioxide partial pressures. According to their results the current density appeared to be limited by gaseous diffusion of CO_2 to the reaction zone.

A one-dimensional thin film model of the porous NiO cathode, where gas phase transport limitations of reactants were discussed on the basis of the 'dusty gas' model, was presented by Jewulski [6]. The calculations showed that molecular diffusion predominates in the gas transport and that gas viscosity was of no practical importance in a typical porous cathode. He also concluded that experimentally measured limiting current densities observed for low oxygen partial pressures could be greatly influenced by the gas phase transport limitations, and that relatively high carbon dioxide partial pressures are more important to prevent gas phase transport limitations. However, at standard gas composition and moderate current densities, the gas transport limitations can be neglected in practice. To study the effect of oxidant composition on the MCFC cathode performance theoretically, a model was made by Kunz and Murphy [7]. While modelling the effects of liquid-phase diffusion, gas-phase diffusion through the cathode and gas-phase diffusion in the cathode plane were also included. The latter effect is due to the fact that incoming gas is fed through a perforated plate, that is, some areas of the cathode are blocked by the closed area of the current collector and can receive reactants only by diffusion in the cathode plane, Fig. 1.

The purpose of this paper is to elucidate to what extent mass transfer limitations in the gas phase will affect the performance of porous cathodes. Experimental data from state-of-the-art porous nickel oxide cathodes in a laboratory cell unit and calculated data are presented. Diffusion coefficients for oxygen and carbon dioxide in gaseous phase are well known, hence accurate calculations of the mass transport through current collector orifices and electrode may be carried out. One and two-dimensional models for the current collector and electrode region have been used. Unlike the model above [7], in which only shielding effects of the current collector are taken into account, we present calculations including the gas-phase mass transfer through the thickness of the current collector. The influence of conversion on the results in the laboratory cell unit are also examined. The mass balance in the gas phase is taken into account by using the Stefan–Maxwell equation. For the one-dimensional calculations a homogeneous agglomerate model is used to describe the microstructure [8, 9]. In this model the effect of conversion of gas in the cell is included. In the two-dimensional model the mass balance in the pore electrolyte is included by using a heterogeneous agglomerate model for the microstructure [10].

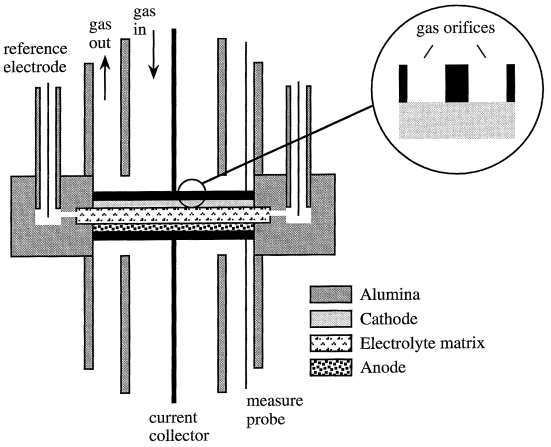

Fig. 1. Schematic drawing of the laboratory cell unit used for electrochemical measurements.

2. Experimental details

The fuel cell used for this investigation was a laboratory cell unit of geometric area $3\,cm^2$. The cell configuration is circular and the incoming gas flows through the orifices in the current collector, perpendicularly to the electrode plane, Fig. 1. Polarization curves were obtained using a Solartron 1286 electrochemical interface. Correction for ohmic drops within the system used the current-interrupt technique. Measurements were performed with three different cathode gases. The partial pressure of oxygen varied while carbon dioxide partial pressure was maintained at 30%. All mixtures were balanced with nitrogen. The anode gas ($80\%H_2$:$20\%CO_2$, humidified at 60 °C) and the reference electrode gas ($67\%CO_2$:$33\%O_2$) were the same throughout the experiments.

3. Derivation of the model equations

The overall reaction of the porous cathode is given by

$$O_2 + 2CO_2 + 4e^- = 2CO_3^{2-} \qquad (1)$$

The reactants enter the electrode through the gas orifice. The MCFC electrodes are given a biporous structure to allow for a penetration of gas throughout the electrode in the larger pores and a subsequent diffusion in the smaller electrolyte filled pores to the electrode surface. A detailed description of the overall processes in the electrode will include gas phase diffusion through gas orifices and the macropores of the electrode, diffusion of dissolved species in the melt and the electrode reaction on the electrode surface; these, together with the conduction of current in pore electrolyte and solid electrode, determine the potential distribution in the electrode.

To simplify the formulation of the model, thus also the solution, some assumptions are introduced. It is assumed that it is possible to describe the three-phase structure of the electrode as a pseudo-homogeneous phase [11]. The effective transport properties, conductivities and diffusivities of this hypothetical phase are functions of the porosity of the porous structure. The system is at constant atmospheric pressure and at steady-state. When taking into account diffusion in the holes of the current collector, the gas is assumed to be at constant pressure. The mechanism for the oxygen reduction reaction in the cathode has still to be clarified. For the calculations the superoxide mechanism for the reduction of oxygen is used [12–14]. Ohm's law is used for the potential distribution in the solid phase of the porous electrode and in the pore electrolyte. The contribution to the total ionic current from the diffusing species is neglected.

These assumptions have been used in the literature [6, 15, 16]. The kinetic equation used is of the Butler–Volmer type with a cathodic transfer coefficient of 1.5, which, coupled to film diffusion of superoxide ions, gives a linear polarization curve in agreement with experimental data [17]. The reference state used for the calculation of the overpotential is the gas composition at the gas inlet, that is, the concentration overpotential is included in the definition of the overpotential [8, 10, 18, 19]. Using this procedure, the influence of the concentration of species in the melt on the exchange current density is introduced.

From the assumptions listed above it is possible to formulate a mass and charge balance for the gas orifices and porous cathode, respectively. For the transport of species in the gas phase the Stefan–Maxwell equation is used [20]:

$$\nabla x_i = \sum_{j=1}^{n} \frac{RT}{PD_{ij}^{\text{eff}}} \left(x_i \boldsymbol{N}_j - x_j \boldsymbol{N}_i \right) \tag{2}$$

Here $\boldsymbol{N}_i$ is the flux vector, x is the mole fraction, $D_{ij}^{\text{eff}} = \varepsilon^{1.5} D_{ij}$ is the effective binary diffusion coefficient of species i–j [20] and P the total pressure. A mass balance for the species O_2 and CO_2 is given by the following expression:

$$-\nabla \cdot \boldsymbol{N}_i - \frac{s_i g\left(x_{i,j}, \Phi_s, \Phi_l\right)}{nF} = 0 \quad \text{in } \Omega \tag{3}$$

Here, the source function g that gives the current production per volume unit is obtained from the micromodel. The function g depends on the composition of the gas phase, $x_{i,j}$, the potential in the pore electrolyte and the catalyst phase, Φ_l and Φ_s respectively. F denotes Faraday's constant, s_i the stoichiometric coefficient of the ith reactant and n the number of electrons in the electrochemical reaction.

The stoichiometry of the overall reaction, at steady state conditions, gives

$$\boldsymbol{N}_{O_2} = \tfrac{1}{2}\, \boldsymbol{N}_{CO_2} \tag{4}$$

The nitrogen present is inert and is neither produced nor consumed in the electrode. That is,

$$\boldsymbol{N}_{N_2} = 0 \tag{5}$$

Furthermore, from the definition of mole fraction,

$$x_{O_2} + x_{CO_2} + x_{N_2} = 1 \tag{6}$$

For the balance of oxygen, Equations 2–6 gives:

$$-\nabla \cdot \left(\left(x_{O_2} \left(\frac{2}{D_{O_2,CO_2}^{\text{eff}}} + \frac{1}{D_{O_2,N_2}^{\text{eff}}} \right) + x_{CO_2} \left(\frac{1}{D_{O_2,N_2}^{\text{eff}}} - \frac{1}{D_{O_2,CO_2}^{\text{eff}}} \right) - \frac{1}{D_{O_2,N_2}^{\text{eff}}} \right)^{-1} \frac{P}{RT} \nabla x_{O_2} \right) - \frac{g\left(x_{i,j}, \Phi_s, \Phi_l\right)}{4F} = 0 \quad \text{in } \Omega \tag{7}$$

and for carbon dioxide

$$-\nabla \cdot \left(\left(x_{O_2} \left(\frac{1}{D_{CO_2,N_2}^{\text{eff}}} - \frac{1}{D_{CO_2,O_2}^{\text{eff}}} \right) + x_{CO_2} \left(\frac{1}{2D_{CO_2,O_2}^{\text{eff}}} + \frac{1}{D_{CO_2,N_2}^{\text{eff}}} \right) - \frac{1}{D_{CO_2,N_2}^{\text{eff}}} \right)^{-1} \times \frac{P}{RT} \nabla x_{CO_2} \right) - \frac{g\left(x_{i,j}, \Phi_s, \Phi_l\right)}{2F} = 0 \quad \text{in } \Omega \tag{8}$$

For the gas orifice the same equations are valid, but with $g = 0$.

To solve Equations 7 and 8, a charge balance has to be formulated since the potential distribution is included in the source term. A charge balance for the system in combination with Ohm's law gives for the solid phase

$$\nabla^2 \Phi_s - \frac{g\left(x_{i,j}, \Phi_s, \Phi_l\right)}{\kappa_s^{\text{eff}}} = 0 \quad \text{in } \Omega \tag{9}$$

and for the pore electrolyte

$$\nabla^2 \Phi_l + \frac{g\left(x_{i,j}, \Phi_s, \Phi_l\right)}{\kappa_l^{\text{eff}}} = 0 \quad \text{in } \Omega \tag{10}$$

3.1. *Two-dimensional model*

The unit cell of an electrode with a current collector is hexagonal seen from the gas inlet. In the two-dimensional model this hexagonal geometry is approximated by a circle, see Fig. 2. This gives a cylindrical geometry for the unit cell of the electrode that makes it possible to introduce rotational symmetry. The current collector geometry is then introduced in the boundary conditions. Along the boundary toward the anode, the potential is assumed to be constant. These assumptions are similar to those given in a previous publication [11] except that, in this paper, the mass transport in the gas phase is included in the mass balance.

The source function g is obtained using a heterogeneous agglomerate structure [10]. The effective diffusivities of the gas orifice are given by $D_{ij}^{\text{eff}} = D_{ij}$. The fluxes of gas in the area of the gas orifice are

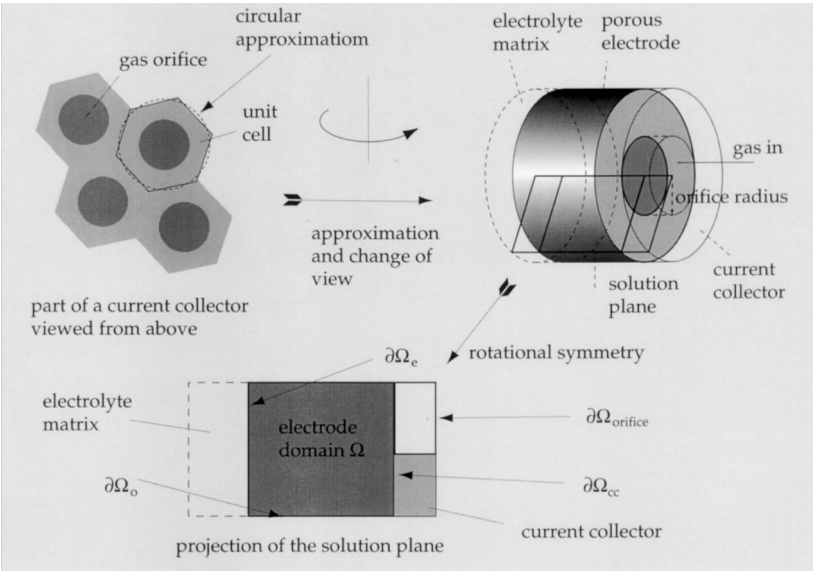

Fig. 2. The unit cell of the current collector seen from above. In the two-dimensional model it is approximated with a circular unit cell to obtain a cylindrical electrode geometry and introduce rotational symmetry.

determined implicitly by the total rates of consumption or production in the electrode domain. One of the boundary conditions for the mass transport equations is

$$x_i = x_i^{\mathrm{b}} \quad \text{at } \partial\Omega_{\mathrm{orifice}} \tag{11}$$

This implies that the partial pressure of the diffusing species is known at the back of the current collector, the boundary denoted $\partial\Omega_{\mathrm{orifice}}$. For the other boundaries, $\boldsymbol{n}$ denoting its normal, the flow of reactants out from the unit cell is set to zero

$$\nabla x_i \cdot \boldsymbol{n} = 0 \quad \text{at } \partial\Omega_{\mathrm{cc}}, \partial\Omega_{\mathrm{e}}, \partial\Omega_{\mathrm{o}} \tag{12}$$

In the two-dimensional model, this is due to rotational symmetry along the rotation axis of the unit cell. A unit cell is equal to its neighbour and thus no composition gradients should be present across its boundary. Equation 12 is valid at the outer surface and at the boundary towards the symmetry axis of the unit cylinder, which are denoted $\partial\Omega_{\mathrm{o}}$. At the boundary towards the electrolyte matrix there is no production or consumption of reactants and neglecting the diffusion across the matrix compared to the consumption inside of the electrode gives Equation 12 also at this boundary, denoted $\partial\Omega_{\mathrm{e}}$. At the boundary towards the current collector, $\partial\Omega_{\mathrm{cc}}$, the transport of reactants is hindered by the current collector itself and thus Equation 12 is valid.

The boundary conditions for the charge balance equations are

$$\Phi_{\mathrm{s}} = \Phi_{\mathrm{s}}^0 \quad \text{at } \partial\Omega_{\mathrm{cc}} \tag{13}$$

and

$$\nabla\Phi_{\mathrm{s}} \cdot \boldsymbol{n} = 0 \quad \text{at } \partial\Omega_{\mathrm{e}}, \partial\Omega_{\mathrm{o}}, \partial\Omega_{\mathrm{orifice}} \tag{14}$$

for the solid phase. For the pore electrolyte the following expressions are valid

$$\Phi_{\mathrm{l}} = \Phi_{\mathrm{l}}^0 \quad \text{at } \partial\Omega_{\mathrm{e}} \tag{15}$$

and

$$\nabla\Phi_{\mathrm{l}} \cdot \boldsymbol{n} = 0 \quad \text{at } \partial\Omega_{\mathrm{cc}}, \partial\Omega_{\mathrm{o}}, \partial\Omega_{\mathrm{orifice}} \tag{16}$$

The system of equations, Equations 7–10, is a coupled system of partial differential equations. The system is solved using the corresponding boundary conditions. The solution method chosen for this problem for the two-dimensional model is a finite element method using rotationally invariant base functions [10, 11]. Values for the parameters used in the models are listed in Table 1.

3.2. *One-dimensional model*

In the one-dimensional model only variations along the depth of the electrode are considered. The current collector is treated as a pseudo-homogeneous porous plate, with transport properties defined by effective diffusion coefficients. This means that the boundary condition (Equation 11) is valid all over the back of the current collector. A homogeneous agglomerate model [9] with spherical agglomerates (agglomerate radius = 5 μm) is used, defining the source function g. The electrolyte film is assumed to have a thickness of 0.04 μm. Kinetic data are the same as in the micromodel used to generate the source term in the two-dimensional model. The equations are transformed into an initial value problem by using a shooting technique and solved by a fourth-order Runge–Kutta procedure. The conversion in the laboratory cell is taken into account in the calculations by assuming that the gas volume outside the current collector behaves like an ideally mixed reactor. The composition at the back of the electrode, Equation 11, will be the same as the outlet concentration of the cell and will

Table 1. Input parameters used in the calculations

Superoxide reaction mechanism	$O_2^- + 2CO_2 + 3e^- = 2CO_3^{2-}$
Anodic transfer coefficient	1.5
Cathodic transfer coefficient	1.5
Cathodic reaction order of superoxide	1
Anodic reaction order of carbon dioxide	−2
Exchange current density	$i_{0,b} \propto c_{O_2^-,b}^{0.5} \times c_{CO_2,b}^{-1}$
Exchange current density for standard gas	$i_{0,b} = 10\,A\,m^{-2}$
Concentration of superoxide	$c_{O_2^-,b} = K_1 \times p_{O_2}^{0.75} \times p_{CO_2}^{-0.5}$
where the equilibrium constant, K_1, is	$0.05\,mol\,m^{-3}\,atm^{-0.25}$
Concentration of carbon dioxide	$c_{CO_2,b} = K_h \times p_{CO_2}$
where the solubility constant, K_h is	$10\,mol\,m^{-3}\,atm^{-1}$
Diffusion coefficient of superoxide in the melt	$1 \times 10^{-9}\,m^2\,s^{-1}$
Diffusion coefficient of carbon dioxide in the melt	$1 \times 10^{-9}\,m^2\,s^{-1}$
Total pressure	$P = 1$ atm
Binary diffusion coefficients in the gaseous phase	
oxygen, carbon dioxide	$D_{O_2,CO_2} = 1.22 \times 10^{-4}\,m^2\,s^{-1}$
oxygen, nitrogen	$D_{O_2,N_2} = 1.62 \times 10^{-4}\,m^2\,s^{-1}$
carbon dioxide, nitrogen	$D_{CO_2,N_2} = 1.23 \times 10^{-4}\,m^2\,s^{-1}$
Temperature	$T = 923$ K
Electrode thickness	0.8 mm
Gas void fraction of the electrode	0.55
Gas void fraction of current collector	0.35
Effective conductivity in the solid phase	$1500\,\Omega^{-1}\,m^{-1}$
Effective conductivity in the solution	$2.5\,\Omega^{-1}\,m^{-1}$

depend on the total flow rate of gas in the cell and on the total current.

4. Results and discussion

4.1. *Electrochemical measurements*

Figure 3 shows the *iR*-corrected polarization curves for a state-of-the-art NiO cathode. Three different cathode gases are used. The polarization curve for the standard composition (15% O_2 or 70% air, 30% CO_2) shows an almost straight line with no indications of bending even at very large current densities, while lower oxygen contents result in a limiting current behaviour. The bent curves are generally a sign of mass transfer limitations in the system, and could be caused by several factors: mass transfer limitations of dissolved species in the electrolyte film on the agglomerates, mass transfer limitations in the gas phase, a high conversion of reactants in the cell or a combination of these.

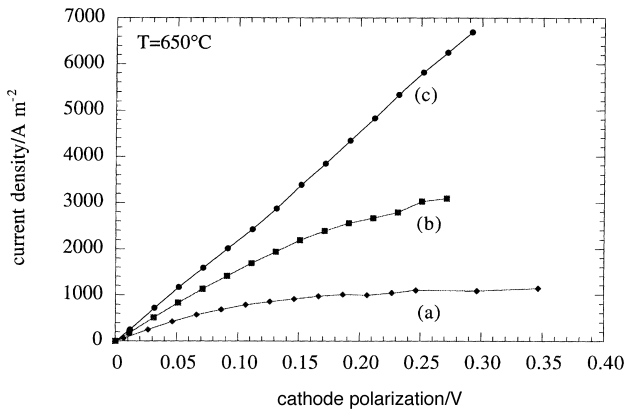

Fig. 3. Cathodic polarization curves for three different gas compositions (a) 1.6%, (b) 5.4% and (c) 15% O_2. All gas mixtures contain 30% CO_2 and are balanced with nitrogen. Gas flow rate is $375\,ml\,min^{-1}$.

An indication that the behaviour is not only caused by transport limitations in the electrolyte is shown in Fig. 4, in which the flow rate of incoming gas (15% O_2) is varied between $70\,ml\,min^{-1}$ and $265\,ml\,min^{-1}$. At higher current densities the polarization curves show a clear dependence on gas flow rate. This should not be the case for the diffusion within the electrolyte film. Increasing the flow rate further does not result in any change in the curve, at least not for 15% O_2. The Figure also shows how the stoichiometric excess of oxygen depends on the current density at different gas flow rates. It is seen that if the conversion of oxidant gas exceeds 10–20% the cathode performance is affected.

To minimize the dependence of polarization curves on gas flow rate, the measurements in Fig. 3 were performed with a flow rate of $375\,ml\,min^{-1}$. Despite the high flow rate, a clear diffusion limitation is seen for lower oxygen contents. For 5.4% O_2 in incoming gas the conversion is estimated to 16% at $3000\,A\,m^{-2}$, and for 1.6% O_2 the conversion becomes 18% at $1000\,A\,m^{-2}$. Thus, the mass transfer limitations observed are at least partly due to the conversion in the laboratory cell.

4.2. *One-dimensional calculations*

In Fig. 5 calculations of the concentration gradients of oxygen through the current collector orifices (0.8 mm thickness, located between dimensionless coordinates −1 and 0) and in the porous cathode (0.8 mm thickness, located between dimensionless coordinates 0 and 1) are shown. The incoming gas contains 15% O_2.

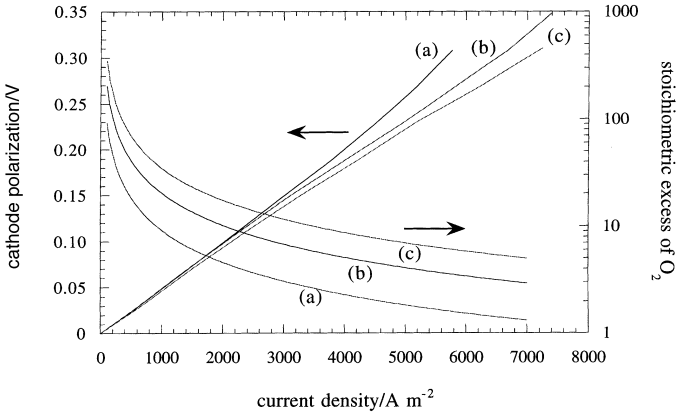

Fig. 4. Cathodic polarization curves and stoichiometric excess of oxygen as function of current density and gas flow rate for standard gas composition. (a) 70, (b) 155 and (c) 265 ml min^{-1}.

For lower current densities (1500 A m^{-2}, dashed line), the effect of gas-phase diffusion is small. However, for larger current densities (4500 A m^{-2}, solid lines), the actual concentration in the electrode becomes much lower than 15% even for high gas flow rates. For the lowest gas flow rate the oxygen partial pressure in the electrode is halved. In these calculations the effect of conversion, as well as diffusion, in the gas orifice has been included. For the standard gas composition the influence of conversion is much larger than the influence of gas phase diffusion in the orifice of the current collector and in the electrode, which is in agreement with the experimental results.

In Fig. 6 the concentration gradients for three different current densities are shown. The concentration of oxygen in incoming gas is 1.6%. At 1500 A m^{-2} (normal operating conditions) the concentration in the electrode becomes very low, resulting in severe mass transfer limitations. This is also experimentally observed (Fig. 3).

The numerical calculations show that the limiting current density observed experimentally to a large extent is due to a limitation of the diffusion rate of oxygen in the gaseous phase rather than in the electrolyte film. For 1.6% oxygen, the influence of mass transfer limitations in the gaseous phase is large even at low current densities, which makes kinetic studies very difficult. Calculations show that the same can be expected for very low carbon dioxide partial pressures.

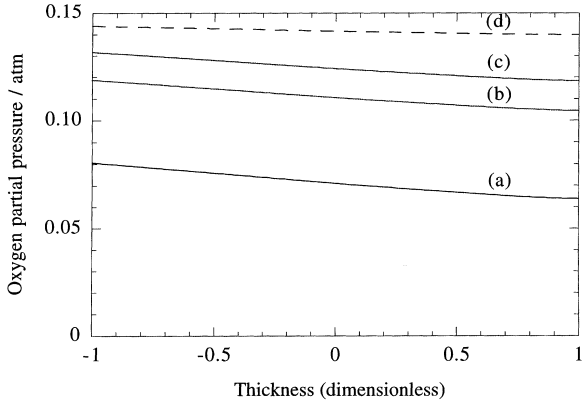

Fig. 5. One-dimensional calculations of the concentration gradients through the current collector (−1,0) and the cathode (0,1) at 1500 (dashed line) and 4500 A m^{-2} (solid line). Oxygen partial pressure of incoming gas is 15%. Gas flow rates are varied between (a) 70, (b) 155, (c) and (d) 265 ml min^{-1}.

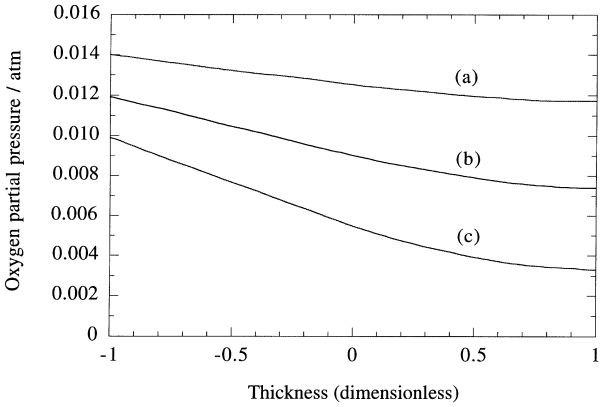

Fig. 6. One-dimensional calculations of the concentration gradients through the current collector and the cathode for varying current densities; (a) 500, (b) 1000 and (c) 1500 A m^{-2}. Incoming gas contains 1.6% oxygen and gas flow rate is 265 ml min^{-1}.

4.3. *Two-dimensional calculations*

The calculated dimensionless oxygen pressure from the two-dimensional simulation in the electrode and current collector, using standard gas composition at a current density of 2040 A m^{-2}, is shown in Fig. 7. The transport through the orifice is assumed to be purely by diffusion. The results are in agreement with the one-dimensional simulations showing negligible concentration gradients for the standard gas composition at normal operating conditions. As already shown, accounting for the mass transport through the gas orifice gives additional gradients in composition before the gas reaches the electrode.

For low reactant partial pressures, the concentration distribution becomes more significant. Figure 8

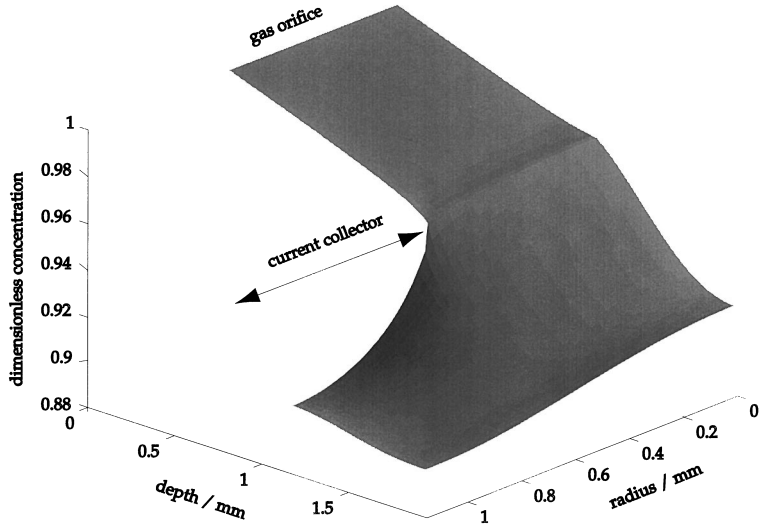

Fig. 7. Two-dimensional calculations of the concentration gradients through the current collector and the cathode. Partial pressure of oxygen is 15%. Current density 2040 A m^{-2}.

shows the dimensionless concentration profile of oxygen for an inlet concentration of 1.6% at 1050 A m^{-2}. The concentration distribution in the direction perpendicular to the current is fairly large; it is, however, smaller than along the depth of the electrode.

To detect the influence on electrode performance of gas transport in lateral direction, the results from the two-dimensional simulations have been compared to the results from the one-dimensional calculations. The difference in performance, due to the lateral diffusion, is quite small. This is explained by the fact that although there are substantial gradients in the lateral direction, due to the nonuniform current distribution most of the current is produced at the outermost part of the electrode where the gradients in composition along the depth of the electrode are more significant, see Fig. 8. If the current distribution becomes more uniform along the depth of the electrode, the significance of the gas transport in the lateral direction is expected to increase. This is also expected when thinner electrodes are used. In the calculations of the concentration gradients in the gaseous phase, the effective binary diffusion coefficients used are quite large. This is due to the assumptions made about the gas void fraction in the electrode and the tortuosity $\left(\tau = \varepsilon^{-0.5}\right)$. A decreased porosity and/or increased tortuosity would result in even larger transport limitations in the electrode.

5. Conclusions

For standard gas composition and normal operating current density, the effect of gas-phase diffusion is small. For low oxygen partial pressures, the influence of mass transfer limitations is large even at low current densities, which makes kinetic studies very difficult. The same can be expected for low carbon

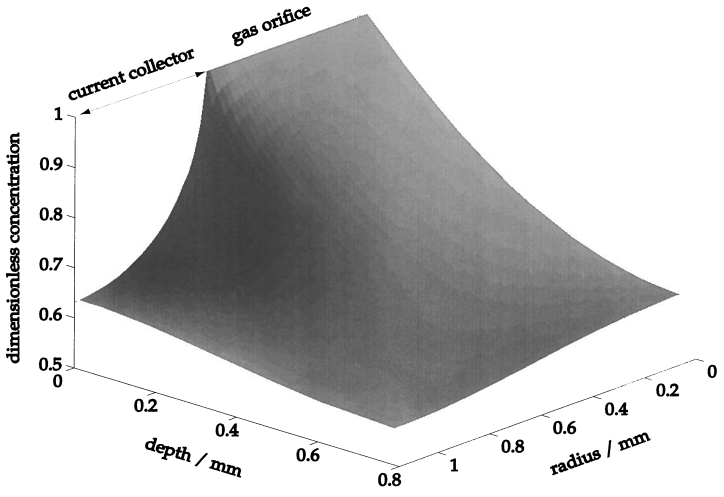

Fig. 8. Two-dimensional calculation of the concentration gradients inside the cathode for a low reactant partial pressure, 1.6% O_2, at 1050 A m^{-2}.

dioxide partial pressures, since the diffusion coefficient for carbon dioxide is of the same order of magnitude as for oxygen. To achieve desirable higher power density than today, operation at current densities exceeding $1500\,A\,m^{-2}$ will be required. In such case the diffusion in the gaseous phase must be considered.

To eliminate the influence of conversion on polarization curves recorded on laboratory cell units, measurements should always be performed with at least a five to ten fold stoichiometric excess of oxygen and carbon dioxide.

Two-dimensional calculations show rather large concentration gradients perpendicular to the current close to the current collector. However, these gradients are much smaller close to the electrolyte matrix. The influence of the gradients in lateral direction on electrode performance is small, which is explained by the fact that most of the current is produced close to the electrolyte matrix.

Acknowledgements

This work is financially supported by the Swedish National Board for Industrial and Technical Development (NUTEK). The laboratory cell unit and cell components are purchased from ECN in the Netherlands.

References

[1] C. Y. Yuh and J. R. Selman, *J. Electrochem. Soc.* **138** (1991) 3642.
[2] S. H. Lu and J. R. Selman, *J. Electroanal Chem.* **333** (1992) 257.
[3] T. Nishina, I. Uchida and J. R. Selman, *J. Electrochem. Soc.* **141** (1994) 1191.
[4] L. J. Bregoli and H. R. Kunz, *ibid.* **129** (1982) 2711.
[5] J. L. Weaver and J. Winnick, *ibid.* **130** (1983) 20.
[6] J. Jewulski, *J. Appl. Electrochem.* **16** (1986) 643.
[7] H. R. Kunz and L. A. Murphy, *J. Electrochem. Soc.* **135** (1988) 1124.
[8] E. Fontes, C. Lagergren and D. Simonsson, *Electrochim. Acta* **38** (1993) 2669.
[9] C. Lagergren, G. Lindbergh and D. Simonsson, *J. Electrochem. Soc.* **142** (1995) 787.
[10] E. Fontes, M. Fontes and D. Simonsson, *Electrochim. Acta* **40** (1995) 1641.
[11] *Idem*, *ibid.* **41** (1996) 1.
[12] A. J. Appleby and S. B. Nicholson, *J. Electroanal. Chem.* **53** (1974) 105.
[13] *Idem*, *ibid.* **83** (1977) 309.
[14] *Idem*, *ibid.* **112** (1980) 71.
[15] H. R. Kunz, L. J. Bregoli and S. T. Szymanski, *J. Electrochem. Soc.* **131** (1984) 2815.
[16] C. Y. Yuh and J. R. Selman, *ibid.* **131** (1984) 2062.
[17] E. Fontes, C. Lagergren and D. Simonsson, submitted to *J. Electroanal. Chem.*
[18] R. Makkus, 'Electrochemical Studies on the Oxygen Reduction and NiO(Li) Dissolution in Molten Carbonate', PhD thesis, TU-Delft, Delft, The Netherlands (1991).
[19] J. S. Newman, Electrochemical Systems, 2nd edn, Prentice Hall, Engelwood Cliffs, NJ (1991).
[20] R. B. Bird, W. E. Stewart and E. N. Lightfoot, 'Transport Phenomena', J. Wiley & Sons, New York (1960).